Available online at www.sciencedirect.com

SCIENCE DIRECT®

Earth and Planetary Science Letters 224 (2004) 509–527

EPSL

www.elsevier.com/locate/epsl

Opal sedimentation shifts in the World Ocean over the last 15 Myr

Giuseppe Cortese*, Rainer Gersonde, Claus-Dieter Hillenbrand[1], Gerhard Kuhn

Alfred Wegener Institute for Polar and Marine Research (AWI), Columbusstrasse, P.O. Box 120161-27515 Bremerhaven, Germany

Received 22 October 2003; received in revised form 20 May 2004; accepted 25 May 2004

Abstract

Biogenic silica (opal) accumulation records were used to trace mechanisms, consequence, and geographic pattern of shifts in the main locus of opal deposition of the World Ocean over the last 15 Myr. Over this time interval, the main opal "sink" seems to have moved from the North Atlantic, to the Pacific, equatorial Pacific, eastern equatorial Pacific, eastern boundary current upwelling systems (California, Namibia, Peru), and finally to the Southern Ocean. The interplay between opal deposition and a series of climatic, tectonic, oceanographic, and biologic events has been analyzed and discussed. These events include the Cenozoic global cooling trend, intensified glaciation in Antarctica, Late Miocene–Early Pliocene biogenic bloom, development of Northern Hemisphere Glaciation (NHG), closing of the Panama Seaway, transition of the climate system from a monopolar- to a bipolar-glaciated world, Mid-Pleistocene Revolution (MPR), nutrient availability, evolution of diatoms and C4 plants, and changes in continental weathering rates. While the observed shifts are mostly traceable to oceanic reorganizations and global climatic evolution, conditions favorable to opal deposition involve the above-mentioned complex mix of processes. For this reason, the interpretation of opal deposition records might not always be straightforward. We, however, believe that it can still provide clear indications of large-scale oceanographic reorganizations in the geological past.

Keywords: opal; Southern Ocean; Mid-Pleistocene Revolution; upwelling; Neogene; glaciation

1. Introduction

Large-scale oceanic circulation has a direct impact on opal deposition (Fig. 1), as the estuarine Pacific (exchange of surface, nutrient-poor, for deep, nutrient-rich, waters) and anti-estuarine Atlantic Ocean circulations are favoring the production/preservation of silica and carbonate, respectively [1]. The effects of this basin to basin fractionation are both on opal preservation, as Pacific bottom waters are less silica unsaturated compared to the Atlantic ones, and production, as Si/N and Si/P ratios increase from the Atlantic to the Pacific/Southern Ocean, thus favoring opal versus carbonate producers [2].

This configuration leads today (Fig. 1) to the localization of opal burial mostly in the equatorial Pacific, in the eastern boundary current upwelling systems, and in the Southern Ocean. The latter accounts for 17–37% of the global opal burial [3], a somewhat conservative estimate compared to previous studies, which attributed up to two-thirds of the opal burial to the Southern Ocean [4]. This observa-

* Corresponding author. Tel.: +49-471-48311207; fax: +49-471-48311149.

[1] Present address: British Antarctic Survey, High Cross, Madingley Road, Cambridge CB3 OET, UK.

E-mail address: gcortese@awi-bremerhaven.de (G. Cortese).

0012-821X/$ - see front matter © 2004 Elsevier B.V. All rights reserved.
doi:10.1016/j.epsl.2004.05.035

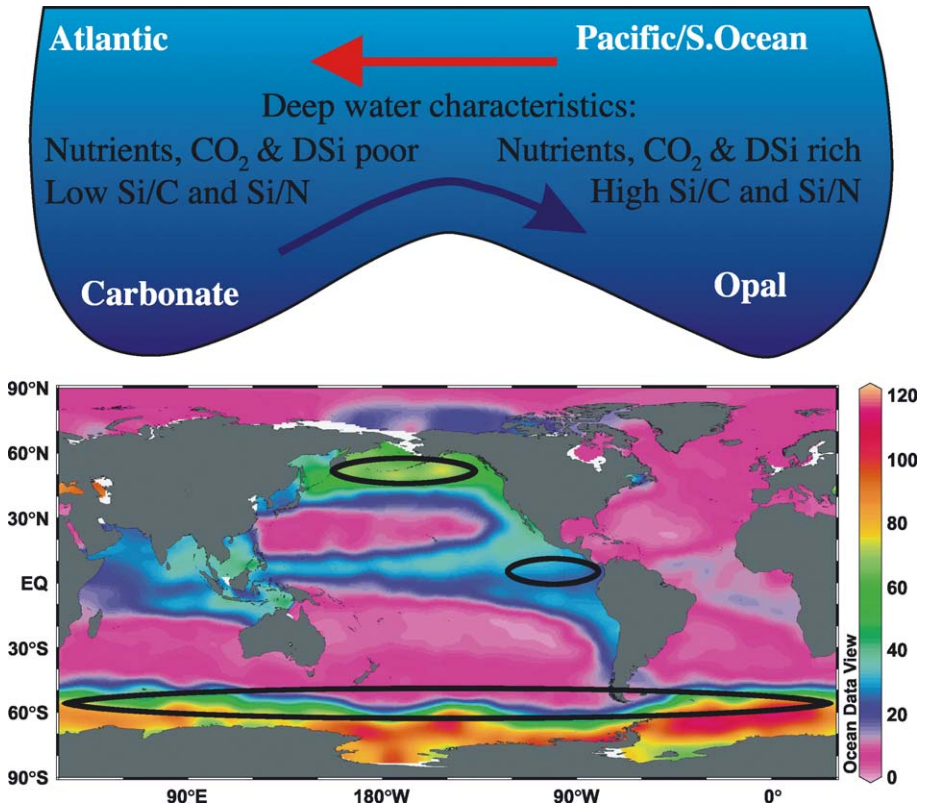

Fig. 1. General ocean circulation and opal sinks. (Top) The general circulation between Atlantic and Pacific/Southern Ocean modified after [1]. Deep waters in the Pacific/Southern Ocean are enriched in nutrients, carbon dioxide, and DSi, and at the same time display higher Si/C and Si/N ratios [2] compared to the Atlantic Ocean. (Bottom) The silica-rich Pacific/Southern Ocean is recognizable in the annually averaged DSi (in μM) distribution at 250-m depth [31]. Black ellipse = modern opal sink.

tion places a particular stress on the importance of opal deposition on continental margins, which might account for the difference [5]. Today, large-scale oceanic circulation therefore has the potential to affect opal deposition by:

(1) "distilling" dissolved silica (DSi) into modern Pacific-like oceans (increase in opal preservation);
(2) favoring opal vs. carbonate export (increase in opal production), as changes in nutrient ratios contribute to select diatoms as main producers compared to other (e.g., calcifying) organisms, which in turn have implications on export.

This static picture is, however, not representative for the last 15 Myr, as conditions favorable to opal deposition shift and generate a dynamic picture through time. For this reason, opal sedimentary records can be used to recognize past oceanic reorganizations, as they are mainly shaped by circulation rearrangements (e.g., opening/closing of gateways, intensification of deep water formation) and global climatic evolution (Cenozoic cooling trend, Antarctica and Northern Hemisphere glaciation (NHG)). Similarly, known oceanographic events can help shed light on the mechanisms leading to opal deposition and increase our knowledge of the Si and C cycles. Climate evolution and oceanic circulation are moreover closely connected, as the development of continental ice sheets, ice shelves, and sea-ice alters the strength and flow direction of the global overturning circulation, and also affects the meridional partitioning in the ocean of nutrients essential to opal-producing organisms. The global cooling trend

during the Cenozoic [6], and events such as the development of glaciation in Antarctica [7], the Late Miocene–Early Pliocene biogenic bloom [8], the closing of the Panama Seaway [9], and the Mid-Pleistocene Revolution (MPR [10]), left an imprint on opal deposition records due to the effects they had on oceanic processes.

Diatoms (siliceous primary producers having opaline valves) strongly influence the cycling of silicon and carbon in oceanic ecosystems. They are responsible for 43% of the ocean primary production [4] and may control the export of carbon to the deep ocean. This confers to them the potential to affect changes in atmospheric CO_2 concentrations on a variety of time scales. The effect on CO_2 sequestration in the ocean is more direct than for skeletal formation in carbonate biomineralizers, a process that reduces alkalinity and results in no net removal of CO_2 from the upper ocean during export [11]. The remains of diatoms and other silica-utilizing organisms are found, as opal sediments, in regions that either play a key role in climate (Southern Ocean) or are very sensitive to climate change (Namibia upwelling system). This connection between biogenic silica and organic carbon, coupled with the one order of magnitude better preservation efficiency of the former compared to the latter, makes opal accumulation records very interesting for paleoceanography and paleoclimatology. In this paper, we will use the opal accumulation history of different oceans to trace mechanisms, consequence, and geographic pattern of shifts in the main opal "sinks" of the World Ocean caused by major oceanic and climatic events.

2. Methods

Most of the opal and stratigraphic data presented here were obtained from the Deep Sea Drilling Project (DSDP) and Ocean Drilling Program (ODP) Scientific Results volumes, or from the Pangaea databank (http://www.pangaea.de). Appropriate references to the original data sources are given both in figure captions and Table 1. Additionally, opal data from ODP Leg 177 (ODP Sites 1091 and 1093) are presented here for the first time.

Opal contents of core samples from ODP Legs 175, 177 (Sites 1089 and 1092), and 178 were determined using an automated leaching technique [12] by analyzing the opal-A content in an aliquot of the homogenized dry bulk sediment samples.

Table 1
Opal data

Site	Location	Method	Reference
DSDP Site 66	Equatorial Pacific	1	Moody et al. [82]
DSDP Site 70	Equatorial Pacific	1	compiled by N. Dittert
DSDP Site 73	Equatorial Pacific	1	compiled by N. Dittert
DSDP Site 346	North Atlantic	1	compiled by N. Dittert
DSDP Site 572	Equatorial Pacific	1	Moody et al. [82]
		1	compiled by N. Dittert
DSDP Site 574	Equatorial Pacific	1	compiled by N. Dittert
DSDP Site 586	Equatorial Pacific	1	Moody et al. [82]
ODP Site 642	North Atlantic	2	Bohrmann [83]
ODP Site 643	North Atlantic	2	Bohrmann [83]
		1	compiled by N. Dittert
ODP Site 644	North Atlantic	2	Bohrmann [83]
ODP Site 658	NW Africa (Cape Blanc)	2	Tiedemann [85]
ODP Site 846	East equatorial Pacific	4	Farrell et al. [8]
ODP Site 850	East equatorial Pacific	4	Farrell et al. [8]
ODP Site 882	North Pacific	2	Maslin et al. [21]
ODP Site 1010	California margin	3	Janecek [84]
ODP Site 1018	California margin	3	Janecek [84]
ODP Site 1021	California margin	3	Janecek [84]
ODP Site 1084	SW Africa (Namibia)	4	Pérez et al. [86]
ODP Site 1089	Southern Ocean (Subtropical Front)	5	Kuhn and Diekman [88]
ODP Site 1091	Southern Ocean (Polar Front Zone)	6	This paper
ODP Site 1092	Southern Ocean (Polar Front)	5	Diekmann et al. [45]
ODP Site 1093	Southern Ocean (Polar Front)	6	This paper
ODP Site 1094	Southern Ocean (Antarctic Zone)	6	This paper
ODP Site 1096	Bellingshausen Sea	5	Hillenbrand and Futterer[22]

The source of the opal data discussed in this paper is indicated, along with the original reference, geographic area, and opal determination method, the latter coded as follows: smear slide analysis (1); density separation technique (2); reduction colorimetric technique [14] (3); a modified version of the previous method (4); automated leaching technique [12] (5); x-ray diffraction technique [87] (6).

Silicon was extracted by wet-chemical means with 1 M NaOH, and concentrations of DSi were measured by molybdate-blue spectrophotometry. The proportion of opal was determined by graphical analysis of the absorbance peaks [13]. The reproducibility of the method is better than 2% for opal-rich samples and 4–10% for samples with <10 wt.% opal [12]. The methods used for the other datasets (Table 1) are wet-alkaline digestion, reduction colorimetric technique [14] and its subsequent modifications, density separation, and smear slide analysis. In addition to the leaching technique, at Leg 177, Sites 1091, 1093 and 1094, BSi contents were estimated from the maximal peak height of the broad hump in x-ray diffractograms, calibrated with standard samples [87]. There are large differences in the reproducibility of these methods, and already within wet-alkaline digestion techniques, interlaboratory calibration studies reveal a spread in the measured values according to the concentration and type of solution used in the digestion [15]. Different techniques (and their error margin) are not, however, drastically influencing our discussion, which is based on major shifts in sediment composition, and which does not integrate, in the same record, measurements obtained by different opal determination methods. Age models were computed by linear interpolation between magneto- and biostratigraphic data, while opal accumulation rates (MAR, in g cm^{-2} kyr^{-1}) were calculated by multiplying linear sedimentation rates with the relative abundance of biogenic silica and dry bulk densities. Opal percentages, based on smear slide estimates, and dry bulk densities are given in the JOIDES SCREEN database for four of the sites reported in Table 1. The references to their original opal data are as follows: DSDP Leg 8, Sites 70 and 73 [16]; Leg 38, Site 346 [17]; Leg 85, Site 574 [18]. Opal MAR was calculated by Dittert based on ages assigned to these sites [19]. The resulting opal MAR data are publicly available on the Pangaea databank (data series label: DittertN_2001.13, database ID#: 2157943).

3. Results

Opal sedimentary records from different oceanic provinces illustrate the strong impact that several major tectonic, climatic, and biologic events (Fig. 2) had over last 15 Myr on the opal deposition in the World Ocean (Fig. 3a–e):

- The global cooling trend [6] since ca. 14–16 Ma (Fig. 2);
- Late Miocene–Early Pliocene biogenic bloom event (4.5–7 Ma);
- The progressive shoaling [9] of the Panama Seaway (13–2.7 Ma);
- North Pacific opal breakdown (2.7 Ma);
- Opal deposition increases in upwelling systems in response to high latitude cooling (2.5 Ma) and switches from 40 to 100 kyr glacial–interglacial cycles (MPR, at 0.9 Ma).

3.1. North Atlantic

Opal deposition collapses at 14 Ma (Fig. 3a), in connection with the intensification of Antarctic glaciation and the development of North Atlantic Deep Water (NADW), as both events favored the Atlantic-to-Pacific fractionation of nutrients linked to the establishment of a marked anti-estuarine circulation in the North Atlantic. The latter hindered upwelling of silica-rich Antarctic Bottom Water (AABW) in the North Atlantic, and this water mass, whose formation rate was also probably increased by the peaking glaciation of Antarctica, was instead rerouted to the Indo-Pacific. The opal system in the North Atlantic is only able to partly recover (Fig. 3a) at times when the nutrient/DSi pool gets enriched either globally (at ca. 5 Ma, during the biogenic bloom event, as recorded by a minor rebound at ODP Site 642) or when there is a fractionation that allows nutrient/DSi levels to increase locally (2.7 Ma, Northern Hemisphere Glaciation (NHG) and North Pacific breakdown, as recorded at ODP Site 644).

3.2. Equatorial Pacific Ocean

Repeated opal deposition shifts (Fig. 3b) took place in connection with ice buildup in Antarctica and the presence of "embryonal" ice caps in the Northern Hemisphere: the main focus for biogenic silica deposition moves between east-central (DSDP Site 574) and eastern (DSDP Site 572) Pacific. Sites off this band (DSDP Sites 70 and 73, to the north and south) do not seem to be affected. The same pattern

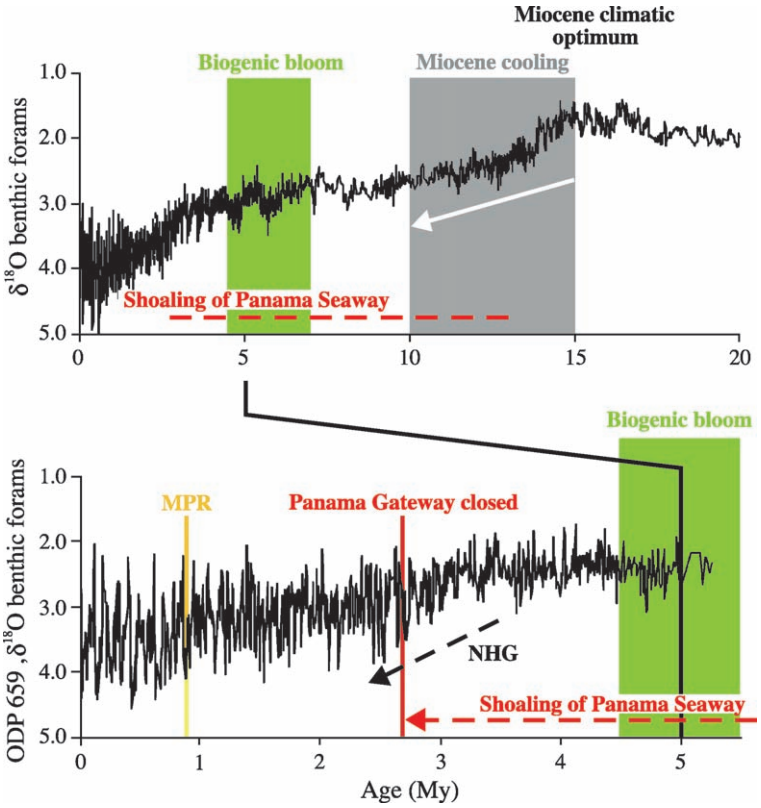

Fig. 2. Neogene climate evolution. General climatic evolution ($\delta^{18}O$ from benthic foraminifera) over the last 20 Myr [6]. The zoomed in portion of the record, last 5 Myr, is from ODP Site 659 [81]. The following events and trends, and the time intervals over which they take place are color-coded as in the ensuing figures (except Fig. 5): Miocene cooling trend, biogenic bloom event, shoaling and closure of the Panama Seaway, intensification of the Northern Hemisphere Glaciation (NHG), the Mid-Pleistocene Revolution (MPR). The Miocene cooling trend (15–10 Ma) is the steep cooling taking place right after the Middle Miocene climatic optimum and is part of the Cenozoic cooling trend. The closure of the Panama Seaway is progressive and culminates at ca. 2.7 Ma. The MPR represents the switch from a 40- to a 100-kyr glacial–interglacial cycle periodicity. The dashed black arrow marked NHG indicates cooling and the onset of major glaciation in the Northern Hemisphere.

repeats itself during the Late Miocene–Early Pliocene biogenic bloom, when changes are strong in the eastern Pacific, but subdued in the central and western side (DSDP Sites 66 and 586).

3.3. East equatorial Pacific

After the biogenic bloom (Fig. 3c–d, horizontal bar), opal MAR drops to almost zero at ODP Site 850, equatorial eastern Pacific, while it remains high post-bloom at ODP 846, Galapagos Basin, easternmost equatorial Pacific, thus resulting in a further opal fractionation within the eastern Pacific, with opal deposition being more and more concentrated toward areas affected by eastern boundary currents. At 4.4 Ma (Fig. 3c–d), the main opal burial area moves from the eastern equatorial Pacific to the Galapagos Basin [8].

3.4. California upwelling system

Major displacements of opal depocenters take place during the circulation changes between 10 and 15 Ma (Fig. 3e), similar to the North Atlantic and equatorial Pacific (Fig. 3a–b). Coastal fractionation (deposition in coastal compared to offshore basins) causes the opal percentage lows at 11.5–10 and 7.6–6.5 Ma [20]. The mechanism behind this coastal fractionation is as follows: a stronger NADW would actually contribute a higher amount of nutrients to the northeastern Pacific and favor upwelling offshore

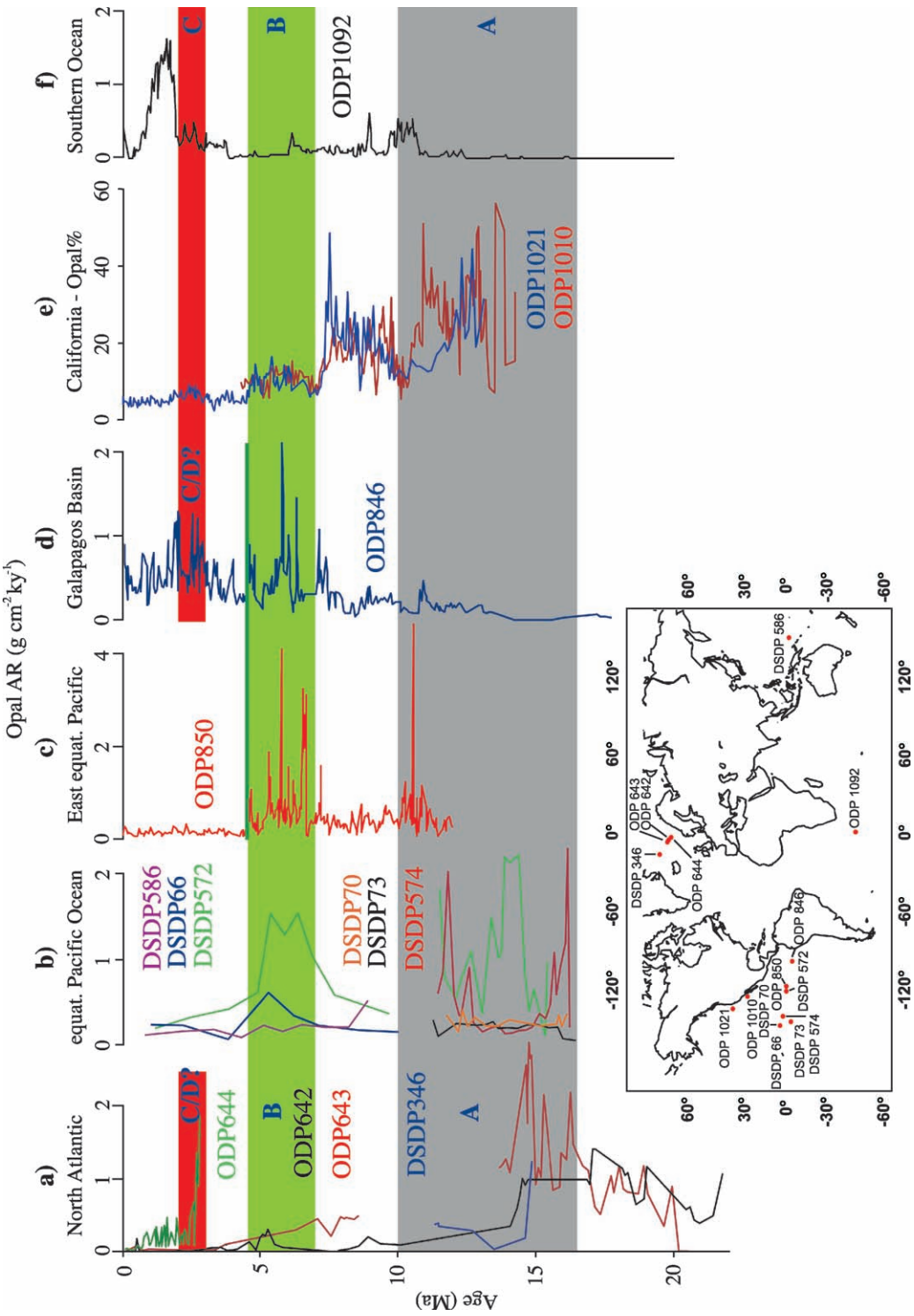
a)
North Atlantic
b)
equat. Pacific Ocean
c)
East equat. Pacific
d)
Galapagos Basin
e)
California - Opal%
f)
Southern Ocean
Opal AR (g cm-2ky-1)
Age (Ma)
C/D?
B
A
C
ODP644
ODP642
ODP643
DSDP346
DSDP586
DSDP66
DSDP572
DSDP70
DSDP73
DSDP574
ODP850
ODP846
ODP1092
ODP1021
ODP1010
DSDP 346
ODP 643
ODP 642
ODP 644
ODP 1021
ODP 1010
DSDP 70
DSDP 66
ODP 850
DSDP 73
DSDP 572
ODP 846
DSDP 574
DSDP 586
ODP 1092

California. However, the presence of low latitudinal temperature gradients, a slower California Current, and a deep nutricline play against, and more than compensate, the potentially increased nutrient availability to shallow waters and result instead in the limitation of nutrient availability offshore [20] and the consequent coastal to offshore fractionation.

The "carbonate crash" recognized at 9.5 Ma in the eastern equatorial Pacific [8] is connected to the start of the progressive shoaling of the Panama Seaway, which strongly affects the characteristics of deep waters entering the Pacific (more carbonate-unsaturated bottom waters), and favors the insaturation of NADW and associated interbasin partitioning of nutrients. Both processes favor opal, as also seen at ODP Sites 1010 and 1021, where opal MAR is on a recovery trend after a minimum at ca. 10 Ma (Fig. 3e).

The shift of opal deposition to the North Pacific and "coastal" Southern Ocean probably caused the opal MAR low observed in California between 4.6 and 2.7 Ma, while the succeeding North Pacific opal breakdown (2.7 Ma) implied, on the contrary, an opal deposition increase along offshore California (Fig. 4). Both the Late Miocene–Early Pliocene biogenic bloom and the opal pulses at 2.5 and 1 Ma (Fig. 4, particularly ODP Site 1018) are well marked and recorded in this upwelling system.

3.5. North Pacific

The opal breakdown dated at ca. 2.7 Ma (Fig. 4) occurs simultaneously with an increase in ice rafted debris deposition [21], suggesting how the NHG caused circulation changes, which probably forced an opal deposition shift to other areas (Southern Ocean, partial recover in North Atlantic).

3.6. Southern Ocean (Bellingshausen and Riiser–Larsen Seas, Atlantic Sector Transect)

Bellingshausen (ODP Sites 1096, and 1101 [22], not shown) and Riiser–Larsen Sea (PS1824-1 [23], not shown) cores display an opal deposition drop at ca. 2.5–3 Ma (Fig. 4). During the same time interval, a sharp change in sedimentary regime had been already recognized in the Weddell Sea and Maud Rise based on a silica- to carbonate-dominated facies shift [24]. Shortly thereafter, at 2 Ma, roughly after the end of the opal breakdown in the North Pacific, and once opal accumulation decreases in upwelling systems, the modern Southern Ocean opal belt is established (Fig. 4) as seen in ODP Leg 177 cores (Sites 1091 and 1093).

3.7. Namibia and Cape Blanc upwelling systems

In the upwelling regimes off NW (Cape Blanc, ODP Site 658) and SW (Namibia, ODP Site 1084) Africa, intense opal MAR pulses are observed between 2 and 3 Ma (Fig. 4). Maxima are also recorded at 1 Ma (Namibia) and 750 ka (Cape Blanc), with the latter event being restricted to the coastal upwelling regime, as it is not present at ODP Site 663 [25], located in the equatorial divergence upwelling.

4. Discussion

4.1. The conveyor belt and silica: today

The aged waters typical for the modern Pacific and Southern Ocean [26] display an increase in the Si/N ratio at intermediate depths, which results in an increase in opal export [2]. The relationship between

Fig. 3. (a–f) Opal history of different oceanic provinces during the last 15 Myr. The Opal records are grouped geographically, as follows: North Atlantic (a), equatorial Pacific Ocean (b), East equatorial Pacific (c), Galapagos Basin (d), California upwelling system (e), Southern Ocean (f). Letters A–D refer to the following events (colors as in Fig. 2): ice buildup in Antarctica and intensified global cooling trend (A), Late Miocene–Early Pliocene biogenic bloom (B), North Pacific opal breakdown and NHG (C), upwelling intensification in connection to high latitude cooling (D). In c–d, the green horizontal line marks the opal shift from the eastern equatorial Pacific to the Galapagos Basin [8]. Note the drop in opal accumulation in the North Atlantic (15 My); the repeated shifts between east–central and eastern Pacific (15–10 My); the repeated coastal-to-offshore fractionations in California (15–7 My); the recovery in most records around the biogenic bloom (4.5–7 My); the fractionation to the Galapagos Basin, easternmost Pacific (4.5 My); the opal drop in the North Atlantic during the oceanic reorganizations connected to NHG (2.7 My); the establishment of opal deposition in the Southern Ocean (2 My). Opal data sources are as follows: DSDP Sites 66, 572, 586 [82]; DSDP Sites 70, 73, 346, 572, 574, ODP Site 643, compiled by Nicholas Dittert, JOIDES SCREEN core data base (http://www.ngdc.noaa.gov/mgg/geology/dsdp/dsdpcdv2.htm), stratigraphy from [19], made publicly available at http://www.pangaea.de; ODP Sites 642, 643, 644 [83]; ODP Sites 846, 850 [8]; ODP Sites 1010, 1021 [84] ODP Site 1092 [45].

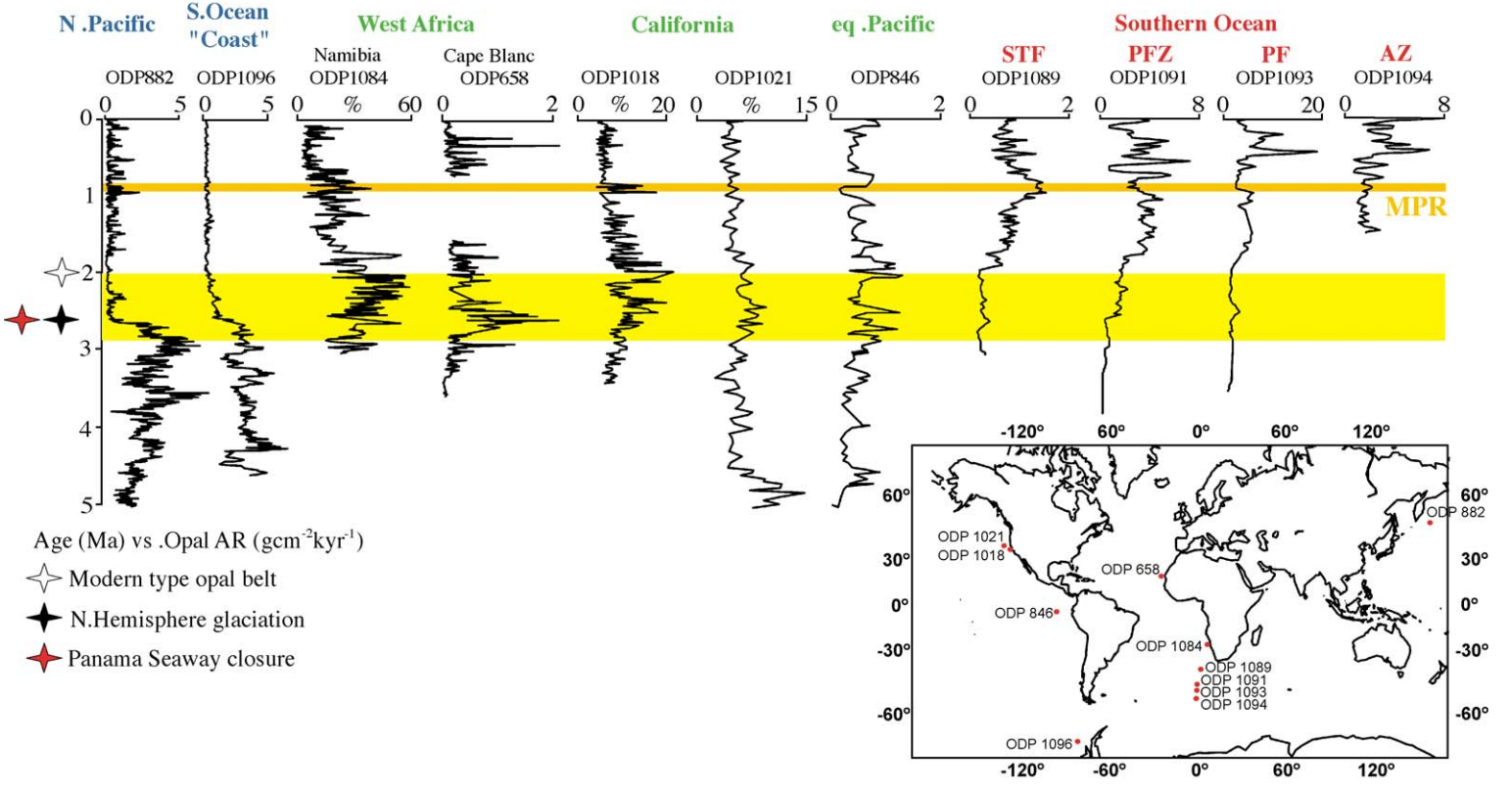

Fig. 4. Shifts of the main opal sink during last 5 My. Opal records from the Southern Ocean (“Coastal” and ACC), North and equatorial Pacific, SW (Namibia) and NW (Cape Blanc) Africa upwelling systems are shown. “Coastal Southern Ocean” includes records from the Bellingshausen and Weddell (not shown) Sea. Additional data sources (not mentioned in Fig. 3): ODP Sites 658 [85], 882 [21], 1018 [84], 1084 [86], 1089 [88], 1091, 1093, 1094 (this paper) and 1096 [22]. The Panama Seaway closure, NHG, the establishment of the modern type opal belt, and MPR are also shown. The roughly 1-My interval covering the shift from North Pacific/Southern Ocean “coast” to upwelling systems, to the Southern Ocean is highlighted in light yellow. STF = SubTropical Front; PFZ = Polar Front Zone; PF = Polar Front; AZ = Antarctic Zone.

opal export and Si/N ratio switches from linear to exponential for Si/N ratios >2, such as one observes in the Southern Ocean and North Pacific. This progressive increase in importance of Si relative to N sets the scene for one of the most important biological players for silica production in the Southern Ocean, as microcosm experiments have demonstrated that diatoms are DSi supercompetitors and dominate other producers above 2 μM DSi [27].

The Southern Ocean and the North Pacific also display maximum BSi/C_{org} flux ratios, and are thus the end members of a general trend observed along the conveyor belt [2], and consisting in an enrichment in BSi, compared to C_{org} export flux. This combined increase in opal preservation and export makes the Southern Ocean the most important "sink" for DSi today. The use of opal proxy records has been criticized because of a strong decoupling between Si and C cycles [28,29], and spatial variations in opal preservation [30]. Moreover, the structure itself of the local ecosystem as well as which diatom species represents the main opal carrier, impacts the generated sedimentary signal. However, opal generally accumulates in sediments when diatom production is high, and therefore the primary signal (related to opal production) is quite relevant in view of the paleoceanographic utilization of opal accumulation data, where emphasis is placed on production rather than on preservation processes. In the modern Pacific and Southern Ocean, intermediate and deep waters are characterized by a higher content in DSi compared to the Atlantic Ocean (Fig. 1). On a first analysis, this suggests that these waters, being less unsaturated in biogenic silica, increase the preservation potential of opal. This is not, however, the case, as the DSi concentration of these waters (up to ca. 170 μM [31]) is well below biogenic silica solubility (ca. 1000 μM [32]). The impact of higher DSi content on BSi dissolution kinetics (due to nonlinearity between dissolution rates and degree of undersaturation [33]) is also to be ruled out, as its effect is more felt at high temperatures (>15–20 °C). Another mechanism, still related to the interbasin differences in DSi, may be more important in increasing the preservation potential of opal: as Atlantic waters are poor in DSi, diatoms tend to be less silicified. This process has a strong influence on the preservation of their frustules as exemplified by a comparison between the Peru and northwest Africa upwelling systems. The dissolution/production ratio is much higher in the Atlantic upwelling [34] than in the Pacific upwelling [35], most probably because the coastal upwelling source waters are much richer in DSi off Peru than off NW Africa.

Through geological time, the conditions leading to the development of a major opal sink are affected by the interaction of many oceanographic, tectonic, and climatic factors that result, at times, in the displacement of the main opal sink from one oceanic province to another. The difficulties in the deconvolution of the influence of global and regional scale processes in shaping opal accumulation records can almost be seen as an inherent characteristic of opal records, as recently illustrated [36]. These authors demonstrate how a similar drop in opal MAR in the Southern Ocean and in the North Pacific may be connected to quite different productivity, nutrient utilization, dust input conditions, but with the unifying tract of representing a transition to a more stable water column structure. In our opinion, the amount of weathering from the continents sets the primary control on the availability of DSi to the ocean, as river runoff represents the main source of DSi to the present-day ocean [4]. The first nutrient screening occurs at continental margins, which are today considered as the site of the missing BSi sink, as the importance of the Southern Ocean opal accumulation has been revised downward [3]. Since the Middle Miocene, the extent of continental margins has not drastically varied, as the breakup of Pangaea, which probably increased the importance of margins in the overall BSi accumulation, was basically completed by then (see also Section 4.4). Major changes in the global DSi budget do not therefore play a role for opal accumulation, even if there are some possible exceptions to this, as the biogenic bloom event (discussed in detail in Section 4.2.2). The character of this event is still, however, debated, as it is not clear whether it represents the consequence of a global increase of nutrient input to the oceans or a change in the distribution of nutrients between basins. Our interpretation of opal accumulation records is therefore mainly in terms of oceanic reorganizations, which displace a relatively constant DSi pool. We will, in the following paragraph, illustrate several examples of this interplay between opal deposition and climatic, tectonic, and biologic events.

4.2. The conveyor belt and silica: examples from the past

4.2.1. Event A: ice buildup in Antarctica and global cooling trend (15 Ma)

The Cenozoic cooling trend [6] and the corresponding decrease in atmospheric CO_2 content are currently interpreted as the cause of Antarctic glaciation [37]. Ice buildup and development of a major Antarctic ice sheet [38] and "embryonal" ice caps in the Northern Hemisphere [39] caused strong ocean circulation rearrangements, with an increase in the flow of Northern Component Water (NCW, the precursor to modern NADW) at 17–15 Ma, enhancing basin to basin nutrient fractionation. Global cooling-related nutrient partitioning between Pacific and Atlantic at ca. 10–12 Ma is also documented in the divergence of the $\delta^{13}C$ curves (derived from benthic foraminifera) relative to these two oceans (Fig. 2 in [6]). During this time interval, opal deposition displays fluctuations in the North Atlantic, equatorial Pacific, and California (Fig. 3a–e), and eventually develops into an opal deposition collapse in the North Atlantic at ca. 15 Ma (Fig. 3a), and a silica switch between the Atlantic and Pacific Ocean in the Middle Miocene at ca. 15 Ma [40]. Predominantly carbonatic and biogenic siliceous sediments accumulated since then in the Atlantic and in the Pacific/Indian Ocean, respectively.

We interpret the silica switch and the opal deposition shifts occurring between 10 and 15 Ma as a consequence of the marked global cooling and the development of a more glaciated globe. The increase in continental ice had a strong impact on deep water formation at high latitudes, particularly in the Southern Ocean, and on regional silica budgets. In fact, both the development of NADW (acting against the upwelling of silica-rich AABW in the North Atlantic [41]) and the increased production of AABW (resulting from increased Antarctic glaciation) enriched the Pacific/Indian Ocean in DSi [40].

4.2.2. Event B: Late Miocene–Early Pliocene biogenic bloom event (4.5–7 Ma)

The Late Miocene–Early Pliocene biogenic bloom event [8] was originally described from the equatorial Pacific and resulted in widespread biogenic deposition, resulting from an increase in oceanic biological productivity. This event could either represent the consequence of shifting ocean circulation patterns, causing nutrient partitioning between the Atlantic and the Pacific Oceans, and therefore not necessarily be connected to a global increase in productivity, or truly represent a global biogenic bloom caused by a global increase in nutrient supply to the ocean. The first hypothesis was based on the observation that at 4.6 Ma an increased deep-ocean circulation with today's pattern (deep water formation in the North Atlantic and Southern Ocean) led to stronger interbasin gradients in nutrients, with lower nutrient concentrations in the Atlantic and higher in the North Pacific [42,43]. Recent studies on phosphorus accumulation rates used as a proxy for biological productivity during the Late Miocene–Early Pliocene from oligotrophic areas of the Indian and Atlantic Oceans [44] seem to suggest how the biogenic bloom occurred on a global rather than a regional scale, and was therefore not linked to a shift of nutrients between oceans, but instead to a worldwide, overall increase in nutrient supply [45]. Further support for this scenario comes from the recognition of the Late Miocene–Early Pliocene biogenic bloom event in other paleoproductivity proxy records from the Indo-Pacific Ocean [43,46,47], the South China Sea [48], based on opal MAR, and the northwest Pacific [49], based on carbonate/organic carbon MAR. A global Late Miocene–Early Pliocene biogenic bloom is also witnessed in the records we present here by partial recovery of the opal system in the North Atlantic (minor rebound at ODP Site 642, Fig. 3a), strong early increases in the equatorial Pacific Ocean, particularly in its eastern part (DSDP Sites 66 and 572, ODP Sites 846 and 850, Fig. 3b–d), a minor recovery of opal abundance in the California upwelling system after the main drop at 7 Ma (ODP Sites 1010 and 1021, Fig. 3e), and variable high opal values in the Southern Ocean (ODP Site 1096, Fig. 4). In most of the presented opal records, particularly those from the Pacific Ocean (Fig. 3b–d), the opal peak is centered between 4.5 and 7 Ma, and may suggest a connection to the preceding drop in opal accumulation displayed in California, causing a remobilization of a DSi pool to the Pacific Ocean (Fig. 3e). Interestingly, this time interval almost coincides with the evolution/spread of C4 plants [50–52], between 7 and 5 Ma, probably in response to low CO_2 concentrations. These plants (mostly weeds) have probably played an important role in controlling both the continental weathering rate

and the total amount of DSi ending up in the ocean by continental runoff. In fact, they favor remobilization of DSi from the enormous continental/soil reservoir by forming siliceous phytoliths that are shedded once the plant dies. They are then easily dissolved, and part of the resulting DSi may move from the continental to the oceanic reservoir.

Other hypotheses for the biogenic bloom event invoke a global scale nutrients increase, linked to the Andean–Himalayan uplift and its impact on stronger continental weathering, leading to higher discharge of nutrients in the ocean [53,54]. Moreover, the rising mountain chains would have also affected atmospheric circulation and precipitation patterns, with the resulting rainfalls providing positive feedback to the higher nutrient levels in rivers and oceans. Additional factors would be the Himalayas blocking of storm tracks from the Indian Ocean at ca. 8 Ma and the consequent intensification of both the Asian monsoon and the associated transfer of nutrients from land to oceans [55].

4.2.3. Event C: North Pacific opal breakdown (2.7 Ma)

The North Pacific opal breakdown (at 2.7 Ma) was probably related [21,56] to the inception of NHG (2.5 Ma), and it could represent the first step in the shift of the main DSi pool from the North Pacific to the pelagic Polar Front area in the Southern Ocean, where it would have led to the development of the ACC opal belt (2 Ma). The mechanism invoked for the opal breakdown [56] is the development, as a consequence of increased NHG, of a strong halocline in the subarctic Pacific, separating nutrient-poor surface waters from nutrient-rich subsurface waters. The reduced input of nutrient-rich subsurface waters to the surface caused reduced productivity. In addition to this, the preservation efficiency of different diatom species plays an important role: the shift from silica to carbonate deposition, already observed in the Weddell Sea at roughly this time [24], is a consequence of the expansion of sea ice and the lower preservation potential of sea-ice adapted diatoms.

As already described for Event A (from 15 Ma, global cooling trend), opal deposition at 2.7 Ma is therefore also affected by an increased cooling event, and here too the control is indirect, taking place through the large-scale oceanographic changes caused by the cooling, and their effect on the distribution of nutrient pools between different ocean basins. An additional important player in further increasing the effectiveness of the conveyor partitioning and establishing regional differences in nutrient pools' availability was a tectonic event: the closure of the Panama Seaway. In fact, the Neogene tectonic closure of the Panama Seaway from 13.0 to 2.7 Ma [9,57] induced deep changes in global thermohaline circulation that might have set the stage for NHG [58,59]. While the link between the closing of the Panama Seaway and NHG is still debated, the shoaling of the Panama Seaway surely implied major oceanographic changes between 4.6 and 4.2 Ma [58]. This resulted in the intensification of NADW formation and, most importantly, the development of the modern salinity and nutrient Atlantic–Pacific contrast, which is reflected in a strong increase in Caribbean/Atlantic carbonate preservation and a complementary strong carbonate dissolution in the Pacific [8,58,60,61]. The different response of carbonate and opal records to large-scale oceanographic changes may be connected to their specific water column unsaturation characteristics, as globally, about half of the BSi redissolves in surface waters, while dissolution starts below the lysocline for carbonate [62]. Opal budgeting studies are in agreement with this observation and show how half (120 Tmol Si yr^{-1}) of the total biogenic silica production is redissolved in the surface-mixed layer [4] and therefore kept available for mineralization by organisms building an opaline silica test. In order for the opal cycle to be strongly affected, an almost complete closure of a passage is therefore necessary, as otherwise this shallow water DSi pool would still be exchanged between two contiguous basins. This is not the case for strong impacts on the carbonate cycle, where already a restricted flow of deep and bottom waters may play an important role in the partitioning of carbonate sediments. This could explain the different response of carbonate and opal depositional events in connection to the progressive shallowing of the Panama Seaway: the observed "Miocene Carbonate Crash" in the eastern equatorial Pacific [8] is an early response triggered by the initial shallowing of the Panama Seaway [63] and is a consequence of the reduced inflow into the Pacific of NADW (substituted by more carbonate-undersaturated southern-source waters), while opal readjustments occur much later, when the passage is severely restricted.

4.2.4. Events D–E: upwelling systems responses (2.5 and 0.9 Ma)

The switch from a monopolar- to a bipolar-glaciated world might be associated with the intensification of high-latitude cooling taking place at ca. 2.5 Ma and causing in turn a strengthening of latitudinal temperature gradients and a stronger upwelling intensity. The MPR, itself a switch from the "40 kyr-" to the "100 kyr-glacial cycles" world, occurred at ca. 0.9 Ma, as documented by benthic foraminifera $\delta^{18}O$ records from ODP Sites 677 and 1085 [64,65]. The gradual global and deep ocean cooling during the Neogene is considered as its possible cause and resulted in a shift in the character of glacial–interglacial cycles from a symmetric, 41-kyr oscillation to an asymmetric, nonlinear, 100-kyr oscillation [66]. Past increases in opal deposition in upwelling systems are observed (Fig. 4) in response to both high latitude cooling at ca. 2.5 Ma and the MPR. Both events might have to do with the development or reorganization of the cryosphere and its increased importance in affecting climate change.

4.3. A scenario for the Southern Ocean–Namibia upwelling opal shift

In order for opal sediments to accumulate on the seafloor, some requirements need to be met, including the presence of nutrients and light conditions necessary for primary producers, a relatively persistent interannual export to the seafloor, and a good preservation efficiency. Sea ice has the potential to disrupt these conditions, and therefore plays an important role in controlling opal deposition in particularly sensitive areas. The expansion of sea ice cover (e.g., during periods of intensified glaciation, like at the onset of NHG, 2.7 Ma) probably terminated opal deposition, mostly due to light limitation of primary producers, and to its association with less well-preserved diatom species. This event is traceable to the North Pacific (ODP Site 882 [21]), the Riiser–Larsen Sea (core PS1824-1 [23]), the Weddell Sea/Maud Rise (cores PS1588-1 and PS1451-1 [23], see also [24]), and the Bellingshausen Sea (ODP Sites 1096 and 1101 [22]). Moreover, the oceanographic readjustments and climate changes connected to NHG led to the environmental push-out and replacement, in the North Pacific and in the coastal Southern Ocean, of diatom assemblages having good preservation efficiency with sea-ice-adapted diatom species having a low preservation efficiency (Fig. 5). Under expanded sea ice conditions, this translates to a DSi in the water column at high latitudes, which is neither used up by primary producers nor definitively sequestered in sediments, and thus remains available, and can even be enriched by remineralization of opaline skeletal remains. This DSi pool becomes instead directly available for upwelling at other locations, as there are intermediate water connections that allow nutrient input to lower latitude areas. Here, upwelling is actually more intense due to the larger gradients in both wind strength and oceanic temperatures under glaciated conditions. The presence of diatom species having high preservation efficiency in the upwelling areas at this time contributes to the realization of the shift, and the

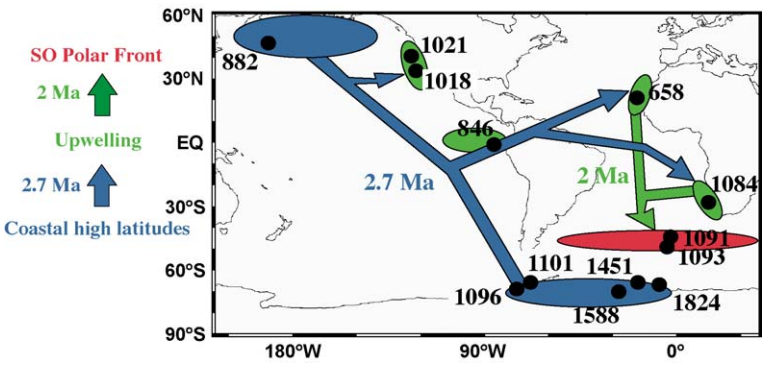

Fig. 5. Establishment of the Southern Ocean Polar Front as the major silica sink. See text (Section 4.3) for explanations and Fig. 4 for data. Additional data sources (not mentioned in Figs. 3 and 4): ODP Site 1101 [22], R/V *Polarstern* cores PS1451-1, PS1588-1, PS1824-1 [23]. Regions are color coded as in Fig. 4.

incorporation of its signal in the sediment, as will also again occur at 2 Ma, when today's opal belt gets established around the Southern Ocean Polar Front (Fig. 4). The earlier drop in opal deposition recorded in sediments from the Riiser–Larsen Sea (core PS1824-1, not shown) and to a lesser extent the Bellingshausen Sea, compared to the North Pacific (Fig. 4), would then reflect the higher sensitivity to sea ice distribution of the Southern Ocean compared to the North Pacific. Caution must be taken, however, in interpreting the data [23] from the Riiser–Larsen Sea (core PS1824-1), as opal percentages and MAR records are slightly shifted in time and could probably be considered synchronous to their North Pacific equivalents. This concept of a DSi pool is similar to what proposed by several recent papers [67–69], on a much shorter time scale: during the Last Glacial Maximum, DSi not exported in a Southern Ocean region could be transferred to other Southern Ocean and/or World Ocean regions. The DSi pool remobilization in this case was not, however, brought about by light limitation, or poorer preservation potential, due to extended ice cover, but rather by the relief of Fe limitation, leading to lower uptake of DSi relative to nitrate and export of unused DSi northward.

A strong cooling took place between 3 and 2.5 Ma, a period encompassing the NHG at 2.7 Ma, but also the shift from a monopolar- to a bipolar-glaciated world at 2.6 Ma. We suggest that, in response to this cooling and to the expanded sea ice cover, opal deposition in the North Pacific and in the "marginal" Southern Ocean (areas close to the Antarctic Peninsula in the Bellingshausen Sea and the Riiser–Larsen Sea) collapsed and never recovered since. The enormous amount of DSi that became available in these two areas ended up (Fig. 5), via intermediate water connections, to the eastern boundary upwelling systems of Namibia, Cape Blanc, and California, where opal deposition bloomed. In fact, Antarctic Intermediate Water and Pacific Intermediate Water were routed, the latter via the Indian Ocean, to the South Atlantic, and gave rise to an interval of increased opal and diatom deposition: Matuyama Diatom Maximum, MDM [70]. Eventually, at ca. 2 Ma, the Polar Front became a site of preference for opal deposition, and in doing so "starved" the Namibia upwelling system of DSi, establishing the ACC opal belt as we know it today. The existence of similar opal export mechanisms in the Benguela upwelling system and the Southern Ocean is documented by the presence of diatom mats in both areas, as if not only the DSi pool, but also an efficient opal export mechanism was inherited by the Southern Ocean from the Benguela upwelling system. Opal accumulation records from the Southern Ocean also display additional strong pulses later than 1 Ma (Fig. 4): these can be related to the latitudinal partitioning of opal within the ACC [71], a consequence of the establishment of the 100-ka glacial/interglacial cyclicity.

The role of DSi in governing the export of biogenic matter to the deep sea has also been discussed on a shorter, glacial–interglacial time scale [72]. Pollock suggests that, during the latest phases of each interglacial, the accelerated melting of the West Antarctic ice sheet provides DSi-enriched deep and intermediate waters to upwelling areas. The resulting enhanced productivity of diatoms at equatorial divergences and coastal upwelling systems leads to higher opal (and carbon) export to the deep sea, causing atmospheric CO_2 drawdown, which acts as a trigger for next glacial. This model (DSi transfer to upwelling areas during late interglacials) is not necessarily in conflict with the scenario we propose above (DSi transfer during increased sea-ice cover in Southern Ocean). In fact, the respective boundary conditions and time scales are different, as no continental ice sheet-related 100-kyr glacial–interglacial cycles were present during pre-MPR time, and while Pollock's model explains remobilization of DSi during a glacial–interglacial cycle, our explanation deals with a long-term sequestration of nutrients away from the Southern Ocean due to its increased, relatively stable, sea-ice coverage.

4.4. Opal shifts in the World Ocean: a synthesis

The sequence of events we propose to explain the observed opal depositional history is as follows (Fig. 2): since the Mid-Miocene climatic optimum (16 Ma), a global cooling trend causes latitudinal gradients to steepen and shift, leading to stronger circulation and upwelling. Large-scale nutrient partitioning is more intense and efficient, and opal deposition becomes more localized into coastal upwelling cells, as originally proposed by [73]. This trend might also have a biological explanation, as the evolution of bloom-forming diatom species peaks in

the Oligocene–Miocene, at a time when the breakup of the Pangaea supercontinent expands the availability and importance of marginal setting habitats, thus increasing opal export efficiency on margins, which is up to five times higher compared to the open ocean [74]. Since the Middle Miocene, occasional episodes of increased weathering and/or availability of nutrients (orogenetic episodes, spreading of terrestrial plants, stronger NADW) cause blooms, preserved in the opal record, where diatoms are able to outcompete other organisms.

A major tectonic event (Panama Seaway closing) contributes to the development of modern opal deposition patterns by blocking off less carbonate-unsaturated bottom water inflow to the Pacific and contributing to the instauration of NADW. Both processes favor opal export and preservation. The intensification of glaciation in Antarctica and the large-scale oceanic circulation reorganization it ignites cause the main DSi pool to move (Figs. 6 and 7) from the Atlantic to the Pacific Ocean. This pool gets then focused in the equatorial Pacific, and post biogenic bloom, it declines in the central equatorial Pacific, compared to the eastern equatorial Pacific, where opal MAR remains high post-bloom [8]. It gets further fractioned to the eastern boundary current upwelling systems with occasional coastal episodes [20]. The North Pacific opal breakdown shifts opal deposition mainly to eastern boundary current upwelling systems, and briefly thereafter, at ca. 2 Ma, the modern Southern Ocean opal belt gets established.

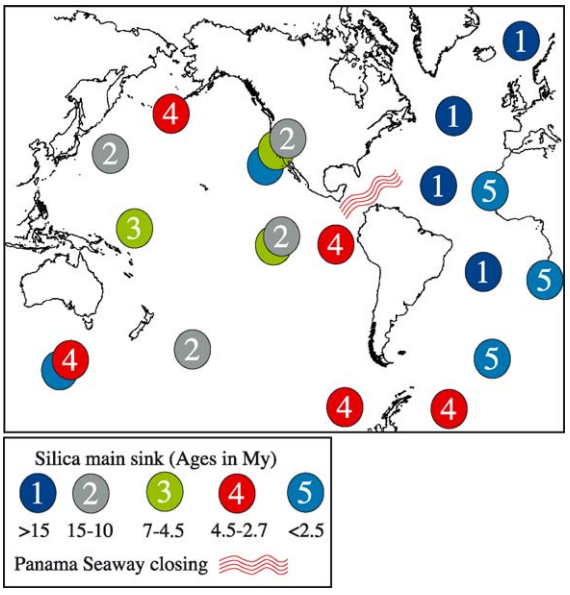

Fig. 6. Schematic summary of the main DSi pool shifts during the last 15 My. A tectonic event (the closing of the Panama Seaway) is also schematically shown. The widespread opal deposition in the Pacific Ocean was most likely caused by the oceanographic changes following an interval of strengthened glaciation on Antarctica.

5. Perspectives

We presented the large-scale evolution of opal deposition through the last 15 Myr and demonstrated how the main DSi sink in the ocean has changed position through time, in response to oceanic conditions quite different from those prevailing today, and leading to the establishment of the Southern Ocean as main silica sink.

There are other factors that should be taken into consideration in order to expand the significance and applicability of the present study, the two most important of which, in our opinion, are the controls on opal dissolution/preservation and the "normalization" of opal MAR in order to correct for sediment focussing. As for the former, the uptake of Al in diatoms has been demonstrated by culture experiments [75] to increase the opal lattice stability and to lead to stronger resistance of opal to dissolution. The opal MAR maxima observed today in the equatorial Pacific may represent a zone with higher than normal aluminum values that would increase the preservation potential of opal while, moving out of the equator, opal MAR, Al contents, and opal preservation potential would decrease [76]. Additional controls of opal dissolution and preservation might also affect the proposed scenarios. In this sense, this study can be improved by further investigations of the cycling of DSi between the deep and surface water compartments, not only in terms of large-scale circulation, but also in order to assess the importance of a series of additional mechanisms for silica dissolution and preservation. These range from the impact of temperature changes on silica dissolution kinetics [33], to bacterial activity and the destruction of organic coatings [77], to the degree of diatom silicification, and to the coupling between pelagic and benthic foodwebs.

The selective accumulation of sediments in sediment drifts might distort the original signal, as the high linear sedimentation rates typical for this setting have an embedding effect on opal, increasing its seabed preservation efficiency [2], i.e., how much of the opal reaching the seafloor is accumulated as sediment. In order to be more accurately interpreted, opal MAR data should therefore be corrected for sediment focussing, in a similar fashion to what is currently done, for more recent sediments, by the application of Thorium excess-based corrections [78]. However, the latter method is not applicable to sediments older than 250–300 ka, and new methods, based on the stable isotope ^{3}He content in interplanetary dust particles, are being developed [79].

The role of different primary producers species also needs to be analyzed in order to assess whether, for example, the observed shifts of opal pools between the North Pacific, the Southern Ocean, and the eastern boundary upwelling systems observed between 3 and 2 Ma might be connected to the appearance/disappearance or evolution of different "opal carriers" in these areas.

Acknowledgements

Funded by the Deutsche Forschungsgemeinschaft as part of the DFG-Research Center "Ocean Margins" of the University of Bremen, No. RCOM0139 and through Grant Ku 683/6. We would particularly like to acknowledge both the SINOPS project [80] and the Pangaea databank (http://www.pangaea.de) for making a great deal of opal data electronically available to the

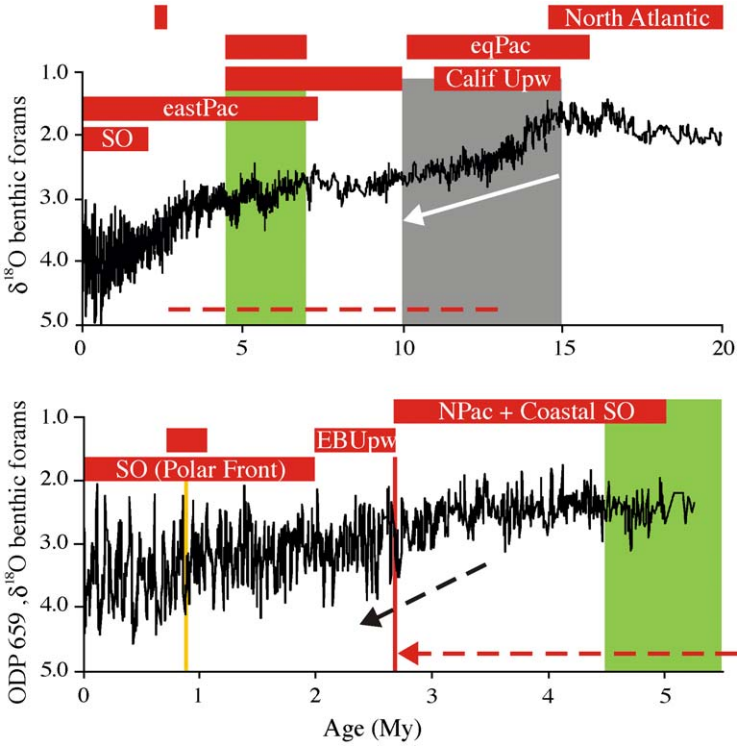

Fig. 7. Summary of opal deposition shifts and events affecting/causing them. Events, trends, and climate records as in Fig. 2. The red bars represent a generalization and possible interpretation of the data seen in Fig. 3 (top half, last 20 My: shift from Atlantic to equatorial Pacific, easternmost Pacific, and Southern Ocean) and Fig. 4 (bottom half, last 5 My: shift from North Pacific/Bellingshausen/Weddell Seas to upwelling systems, and Southern Ocean, mostly Polar Front). EqPac = equatorial Pacific; Calif Upw = California upwelling system; eastPac = easternmost equatorial Pacific; SO = Southern Ocean; Npac + Coastal SO = North Pacific, Bellingshausen and Weddell Seas; EBUpw = eastern boundary currents upwelling systems.

scientific community. Olivier Ragueneau and two anonymous reviewers are thanked for their constructive comments. ***[BARD]***

References

[1] W.H. Berger, Biogenic deep-sea sediments: fractionation by deep-sea circulation, Geological Society of America Bulletin 18 (1970) 1385–1402.

[2] O. Ragueneau, P. Tréguer, A. Leynaert, R.F. Anderson, M.A. Brzezinski, D.J. DeMaster, R.C. Dugdale, J. Dymond, V. Martin-Jézéquel, D.M. Nelson, B. Quéguiner, A review of the Si cycle in the modern ocean: recent progress and missing gaps in the application of biogenic opal as a paleoproductivity proxy, Global and Planetary Change 26 (2000) 317–365.

[3] D.J. DeMaster, The accumulation and cycling of biogenic silica in the Southern Ocean: revisiting the marine silica budget, Deep-Sea Research: Part 2. Topical Studies in Oceanography 49 (2002) 3155–3167.

[4] P. Treguer, D.M. Nelson, A.J. Van Bennekom, D.J. DeMaster, A. Leynaert, B. Quéguiner, The balance of silica in the world ocean: a reestimate, Science 268 (1995) 375–379.

[5] D.J. DeMaster, O. Ragueneau, The preservation of biogenic silica in marine sediments and the role of continental margin deposits in the marine silica budget, in: O. Ragueneau, A. Leynaert, P. Treguer (Eds.), Opaleo: On the Use of Opal as a Paleoproductivity Proxy. Minutes of the First Workshop, Brest, 1996, pp. 68–71.

[6] J. Zachos, M. Pagani, L. Sloan, E. Thomas, K. Billups, Trends, rhythms, and aberrations in global climate 65 Ma to present, Science 292 (2001) 686–693.

[7] P.F. Barker, P.J. Barrett, A.K. Cooper, P. Huybrechts, Antarctic glacial history from numerical models and continental margin sediments, Palaeogeography, Palaeoclimatology, Palaeoecology 150 (1999) 247–267.

[8] J.W. Farrell, I. Raffi, T.R. Janecek, D.W. Murray, M. Levitan, K.A. Dadey, K.-C. Emeis, M. Lyle, J.-A. Flores, S. Hovan, Late Neogene sedimentation patterns in the eastern equatorial Pacific, in: N.G. Pisias, L.A. Mayer, T.R. Janecek, A. Palmer-Julson, T.H. vanAndel (Eds.), Proc. ODP, Sci. Results, Ocean Drilling Program, College Station, TX, 1995, pp. 717–756.

[9] L.S. Collins, A.G. Coates, W.A. Berggren, M.-P. Aubry, J. Zhang, The Late Miocene Panama Isthmian Strait, Geology 24 (1996) 687–690.

[10] W.F. Ruddiman, M. Raymo, A. McIntyre, Matuyama 41,000-year cycles: North Atlantic Ocean and northern hemisphere ice sheets, Earth and Planetary Science Letters 80 (1986) 117–129.

[11] T. Volk, M.I. Hoffert, Ocean carbon pumps: analysis of relative strengths and efficiencies in ocean-driven atmospheric CO_2 changes, in: E.T. Sundquist, W.S. Broecker (Eds.), The Carbon Cycle and Atmospheric CO_2: Natural Variations Archean to Present, AGU, Geophys. Monogr. Ser., Washington, DC, 1985, pp. 99–110.

[12] P.J. Müller, R. Schneider, An automated leaching method for the determination of opal in sediments and particulate matter, Deep-Sea Research 40 (1993) 425–444.

[13] D.J. DeMaster, The supply and accumulation of silica in the marine environment, Geochimica et Cosmochimica Acta 45 (1981) 1715–1732.

[14] R.A. Mortlock, P.N. Froelich, A simple method for the rapid determination of biogenic opal in pelagic marine sediments, Deep-Sea Research: Part 1. Oceanographic Research Papers 36 (1989) 1415–1426.

[15] D.J. Conley, An interlaboratory comparison for the measurement of biogenic silica in sediments, Marine Chemistry 63 (1998) 39–48.

[16] J.I. Tracey Jr., G.H. Sutton, W.D. Nesteroff, J. Galehouse, C.C. von der Borch, T.C. Moore, J.H. Lipps, B.U. Haq, J.P. Beckmann, Initial Reports of the Deep Sea Drilling Project, Volume VIII, Covering Leg 8 of the Cruises of the Drilling Vessel "Glomar Challenger", Honolulu, Hawaii to Papeete, Tahiti, October–December, 1969, U.S. Government Printing Office, Washington, DC, 1971, 1037 pp.

[17] The Shipboard Scientific Party, Sites 346, 347, and 349, in: M. Talwani, G. Udintsev, et al (Eds.), Init. Rep. DSDP XXXVIII, (1976) S21–S94.

[18] L.A. Mayer, F. Theyer, J.A. Barron, D.A. Dunn, T. Handyside, S. Hills, I. Jarvis, C.A. Nigrini, N.G. Pisias, A. Pujos, T. Saito, P.M. Stout, E. Thomas, N. Weinreich, R.H. Wilkens, M.G. Bailey, Initial Reports of the Deep Sea Drilling Project Leg 85, Covering Cruises of the Drilling Vessel Glomar Challenger, Los Angeles, California, to Honolulu, Hawaii, March–April 1982, U.S. Government Printing Office, Washington, DC, 1985, pp. 225–329.

[19] D. Lazarus, C. Spencer-Cervato, M. Pika-Biolzi, J.P. von Salis, K. von Salis, H. Hilbrecht, H. Thierstein, Revised chronology of Neogene DSDP Holes from the World Ocean, Ocean Drilling Program Technical Note 24 (1995), 301 pp.

[20] J.A. Barron, M. Lyle, I. Koizumi, Late Miocene and Early Pliocene biosiliceous sedimentation along the California margin, Revista Mexicana de Ciencias Geológicas 19 (2002) 161–169.

[21] M.A. Maslin, G.H. Haug, M. Sarnthein, R. Tiedemann, The progressive intensification of northern hemisphere glaciation as seen from the North Pacific, Geologische Rundschau 85 (1996) 452–465.

[22] C.-D. Hillenbrand, D.K. Fütterer, Neogene to Quaternary deposition of opal on the continental rise west of the Antarctic Peninsula, ODP Leg 178, Sites 1095, 1096, and 1101, in: P.F. Barker, A. Camerlenghi, G.D. Acton, A.T.S. Ramsay (Eds.), Proc. ODP, Sci. Results, Ocean Drilling Program, College Station, TX, 2001, pp. 1–33, [Online]. Available from World Wide Web: <http://www-odp.tamu.edu/publications/178_SR/VOLUME/CHAPTERS/SR178_023.PDF>.

[23] C.-D. Hillenbrand, W. Ehrmann, Late Neogene to Quaternary environmental changes in the Antarctic Peninsula region: Evidence from drift sediments, Global and Planetary Change (submitted for publication).

[24] A. Abelmann, R. Gersonde, V. Spiess, Pliocene–Pleistocene paleoceanography in the Weddell Sea—siliceous microfossil evidence, in: U. Bleil, J. Thiede (Eds.), Geological History of

the Polar Oceans, Arctic versus Antarctic, Kluwer, Dordrecht, 1990, pp. 729–759.
[25] S. Schneider, Quartäre Schwankungen in Strömungsintensität und Produktivität als Abbild der Wassermassen-Variabilität im Äquatorialen Atlantik (ODP Sites 959 und 663): Ergebnisse aus Siltkorn-Analysen, Berichte Fachbereich Geowissenschaften Univ. Bremen 187, 134 pp.
[26] E. Bard, Correction of accelerator mass spectrometry ^{14}C ages measured in planktonic foraminifera: paleoceanographic implications, Paleoceanography 3 (1988) 635–645.
[27] J.K. Egge, D.L. Aksnes, Silicate as regulating nutrient in phytoplankton competition, Marine Ecology. Progress Series 83 (1992) 281–289.
[28] W.H. Berger, J.C. Herguera, Reading the sedimentary record of the ocean's productivity, in: P.G. Falkowski, A.D. Woodhead (Eds.), Primary Productivity and Biogeochemical Cycles in the Sea, Plenum, New York, 1992, pp. 455–486.
[29] N. Kumar, R.F. Anderson, R.A. Mortlock, P.N. Froelich, P. Kubik, B. Dittrich-Hannen, M. Duter, Increased biological productivity and export production in the glacial Southern Ocean, Nature 378 (1995) 675–680.
[30] D.M. Nelson, P. Trèguer, M.A. Brzezinski, A. Leynaert, B. Quéguiner, Production and dissolution of biogenic silica in the ocean: revised global estimates, comparison with regional data and relationship to biogenic sedimentation, Global Biogeochemical Cycles 9 (1995) 359–372.
[31] M. Conkright, S. Levitus, T. O'Brien, T. Boyer, J. Antonov, C. Stephens, World Ocean Atlas 1998 CD-ROM Data Set Documentation, Silver Spring, MD, 1998, p. 16.
[32] P. Van Cappellen, L. Qiu, Biogenic silica dissolution in sediments of the Southern Ocean: I. Solubility, Deep-Sea Research: Part 2. Topical Studies in Oceanography 44 (1997) 1109–1128.
[33] P. Van Cappellen, L. Qiu, Biogenic silica dissolution in sediments of the Southern Ocean: II. Kinetics, Deep-Sea Research: Part 2. Topical Studies in Oceanography 44 (1997) 1129–1149.
[34] D.M. Nelson, J.J. Goering, Near-surface silica dissolution in the upwelling region off northwest Africa, Deep-Sea Research 24 (1977) 65–73.
[35] D.M. Nelson, J.J. Goering, D.W. Boisseau, Consumption and regeneration of silicic acid in three coastal upwelling systems, in: F.A. Richards (Ed.), Coastal Upwelling, American Geophysical Union, Washington, DC, 1981, pp. 242–256.
[36] D. Sigman, S.L. Jaccard, G.H. Haug, Polar ocean stratification in a cold climate, Nature 428 (2004) 59–63.
[37] R.M. DeConto, D. Pollard, A coupled climate-ice sheet modeling approach to the Early Cenozoic history of the Antarctic ice sheet, Palaeogeography, Palaeoclimatology, Palaeoecology 198 (2003) 39–52.
[38] N.J. Shackleton, J.P. Kennett, Paleotemperature history of the Cenozoic and the initiation of Antarctic glaciation: oxygen and carbon isotope analysis in DSDP Sites 277, 279, and 281, Initial Reports of the Deep Sea Drilling Project, vol. 29, U.S. Government Printing Office, Washington, DC, 1975, pp. 743–755.
[39] J. Thiede, A. Winkler, T. Wolf-Welling, O. Eldholm, A.M. Myhre, K.-H. Baumann, R. Henrich, R. Stein, Late Cenozoic history of the Polar North Atlantic: results from ocean drilling, Quaternary Science Reviews 17 (1998) 185–208.
[40] G. Keller, J.A. Barron, Paleoceanographic implications of Miocene deep-sea hiatuses, Geological Society of America Bulletin 94 (1983) 590–613.
[41] W.H. Berger, E.L. Winterer, Plate stratigraphy and the fluctuating carbonate line, in: K.J. Hsü, H.C. Jenkins (Eds.), Pelagic Sediments on Land and Under the Sea, International Association of Sedimentologists Special Publication, 1973, pp. 11–48.
[42] R. Keir, On the Late Pleistocene ocean geochemistry and circulation, Paleoceanography 3 (1988) 413–447.
[43] G.R. Dickens, R.M. Owen, Sediment geochemical evidence for an early middle Gilbert (early Pliocene) productivity peak in the North Pacific Red Clay Province, Marine Micropaleontology 27 (1996) 107–120.
[44] C.S. Hermoyian, R.M. Owen, Late Miocene–early Pliocene biogenic bloom: evidence from low-productivity regions of the Indian and Atlantic Oceans, Paleoceanography 16 (2001) 95–100.
[45] B. Diekmann, M. Fälker, G. Kuhn, Environmental history of the south-eastern South Atlantic since the Middle Miocene: evidence from the sedimentological records of ODP Sites 1088 and 1092, Sedimentology 50 (2003) 511–529.
[46] L.C. Peterson, D.W. Murray, W.U. Ehrmann, P. Hempel, Cenozoic carbonate accumulation and compensation depth changes in the Indian Ocean, in: R.A. Duncan, D.K. Rea, R.B. Kidd, U. von Rad, J.K. Weissel (Eds.), Synthesis of Results from Scientific Drilling in the Indian Ocean, Am. Geophys. Union Geophys. Monogr, 70 (1992), 311–333.
[47] W.G. Seisser, Paleoproductivity of the Indian Ocean during the Tertiary Period, Global and Planetary Change 11 (1995) 71–88.
[48] J. Li, R. Wang, B. Li, Variations of opal accumulation rates and paleoproductivity over the past 12 Ma at ODP Site 1143, southern South China Sea, Chinese Science Bulletin 47 (2002) 596–598.
[49] G. Mora, Variations in the accumulation of marine organic matter and carbonates at Leg 186 sites, in: K. Suyehiro, I.S. Acton, G.D. Acton, M. Oda (Eds.), Proc. ODP, Sci. Results 186, 2002, pp. 1–17, Online. Available from World Wide Web: <http://www-odp.tamu.edu/publications/186_SR/VOLUME/CHAPTERS/103.PDF>.
[50] T.E. Cerling, Y. Wang, J. Quade, Expansion of C4 ecosystems as an indicator of global ecological change in the Late Miocene, Nature 361 (1993) 344–345.
[51] T.E. Cerling, J.M. Harris, B.J. MacFadden, M.G. Leakey, J. Quade, V. Eisenmann, Global vegetation change through the Miocene–Pliocene boundary, Nature 389 (1997) 153–158.
[52] M. Pagani, K.H. Freeman, M.A. Arthur, Late Miocene atmospheric CO_2 concentrations and the expansion of C4 grasses, Science 285 (1999) 876–879.
[53] M.L. Delaney, G.M. Filippelli, An apparent contradiction in the role of phosphorus in the Cenozoic mass balances for the world ocean, Paleoceanography 9 (1994) 513–527.

[54] D.K. Rea, I.A. Basov, L.A. Krissek, the Leg 145 Scientific Party, Scientific results of drilling the North Pacific Transect, in: D.K. Rea, I.A. Basov, D.W. Scholl, J.F. Allan (Eds.), Proc. ODP, Sci. Results, Ocean Drilling Program, College Station, TX, 1995, pp. 577–596.

[55] G.M. Filippelli, Intensification of the Asian monsoon and a chemical weathering event in the Late Miocene–early Pliocene: implications for the later Neogene climate change, Geology 25 (1997) 27–30.

[56] G.H. Haug, D.M. Sigman, R. Tiedemann, T.F. Pedersen, M. Sarnthein, Onset of permanent stratification in the subarctic Pacific Ocean, Nature 401 (1999) 779–782.

[57] H. Duque-Caro, Neogene stratigraphy, paleoceanography and paleobiogeography in northwest South America and the evolution of the Panama Seaway, Palaeogeography, Palaeoclimatology, Palaeoecology 77 (1990) 203–234.

[58] G.H. Haug, R. Tiedemann, Effect of the formation of the Isthmus of Panama on Atlantic Ocean thermohaline circulation, Nature 393 (1998) 673–676.

[59] N.W. Driscoll, G.H. Haug, A short circuit in thermohaline circulation: a cause for northern hemisphere glaciation? Science 282 (1998) 436–438.

[60] G.H. Haug, R. Tiedemann, R. Zahn, A.C. Ravelo, Role of Panama Uplift on oceanic freshwater balance, Geology 29 (2001) 207–210.

[61] K.G. Cannariato, A.C. Ravelo, Pliocene–Pleistocene evolution of the eastern Pacific surface water circulation and thermocline depth, Paleoceanography 12 (1997) 805–820.

[62] W.H. Berger, Biogenous deep-sea sediments: production, preservation, and interpretation, in: J.P. Riley, R. Chester (Eds.), Treatise on Chemical Oceanography, Academic Press, New York, 1976, pp. 265–388.

[63] K.H. Nisancioglu, M.E. Raymo, P.H. Stone, Reorganization of Miocene deep water circulation in response to the shoaling of the Central American Seaway, Paleoceanography 18 (2003) 1006, doi:10.1029/2002PA000767.

[64] N.J. Shackleton, A. Berger, W.R. Peltier, An alternative astronomical calibration of the Lower Pleistocene timescale based on ODP Site 677, Earth Sciences 81 (1990) 251–261.

[65] A.C. Ravelo, D.H. Andreasen, Enhanced circulation during a warm period, Geophysical Research Letters 27 (2000) 1001–1004.

[66] K.A. Maasch, B. Saltzman, A low-order dynamical model of global climatic variability over the full Pleistocene, Journal of Geophysical Research 95 (1990) 1955–1963.

[67] M.A. Brzezinski, C.J. Pride, V.M. Franck, D.M. Sigman, J.L. Sarmiento, K. Matsumoto, N. Gruber, G.H. Rau, K.H. Coale, A switch from $Si(OH)_4$ to NO^{-3} depletion in the glacial Southern Ocean, Geophysical Research Letters 29 (2002) 1564, doi:10.1029/2001GL014349.

[68] K. Matsumoto, J.L. Sarmiento, M.A. Brzezinski, Silicic acid leakage from the Southern Ocean: a possible explanation for glacial atmospheric *p*CO2, Global Biogeochemical Cycles 16 (2002) 1031, doi:10.1029/2001GB001442.

[69] J.L. Sarmiento, N. Gruber, M.A. Brzezinski, J.P. Dunne, High-latitude controls of thermocline nutrients and low latitude biological productivity, Nature 427 (2004) 56–60.

[70] C.B. Lange, W.H. Berger, H.-L. Lin, G. Wefer, the Shipboard Scientific Party Leg 175, The early Matuyama diatom maximum off SW Africa, Benguela current system (ODP Leg 175), Marine Geology 161 (1999) 93–114.

[71] M. Frank, R. Gersonde, M.R. van der Loeff, G. Bohrmann, C.C. Nürnberg, P.W. Kubik, M. Suter, A. Mangini, Similar glacial and interglacial export bioproductivity in the Atlantic sector of the Southern Ocean: multiproxy evidence and implications for glacial atmospheric CO_2, Paleoceanography 15 (2000) 642–658.

[72] D.E. Pollock, The role of diatoms, dissolved silicate and Antarctic glaciation in glacial/interglacial climate change: a hypothesis, Global and Planetary Change 14 (1997) 113–125.

[73] J.G. Baldauf, J.A. Barron, Evolution of biosiliceous sedimentation patterns—Eocene through Quaternary: paleoceanographic response to polar cooling, in: U. Bleil, J. Thiede (Eds.), Geological History of the Polar Oceans: Arctic Versus Antarctic, Kluwer Academic, Dordrecht, 1990, pp. 575–607.

[74] L.H. Burckle, R. Sambrotto, The Wilson cycle, the rise of bloom-forming diatoms and initiation of Antarctic glaciation: a hypothesis, Geophysical Research Abstracts 5 (2003) 13514.

[75] A.J. van Bennekom, A.G.J. Buma, R.F. Nolting, Dissolved aluminum in the Weddell-Scotia confluence and effect of Al on the dissolution kinetics of biogenic silica, Marine Chemistry 35 (1991) 423–434.

[76] J. Dymond, R. Collier, J. McManus, S. Honjo, S. Manganini, Can the aluminum and titanium contents of ocean sediments be used to determine the paleoproductivity of the oceans? Paleoceanography 12 (1997) 586–593.

[77] K.D. Bidle, F. Azam, Accelerated dissolution of diatom silica by marine bacterial assemblage, Nature 397 (1999) 508–512.

[78] M. Frank, R. Gersonde, M.R. van der Loeff, G. Kuhn, A. Mangini, Late Quaternary sediment dating and quantification of lateral sediment redistribution applying $^{230}Th_{ex}$: a study from the eastern Atlantic sector of the Southern Ocean, Geologische Rundschau 85 (1996) 554–566.

[79] F. Marcantonio, R.F. Anderson, M. Stute, N. Kumar, P. Mix, A.C. Mix, Extraterrestrial ^{3}He as a tracer of marine sediment transport and accumulation, Nature 383 (1996) 705–707.

[80] N. Dittert, L. Corrin, M. Diepenbroek, H. Grobe, C. Heinze, O. Ragueneau, Management of (pale-)oceanographic data sets using the PANGAEA information system: the SINOPS example, Computers & Geosciences 28 (2002) 789–798.

[81] R. Tiedemann, M. Sarnthein, N.J. Shackleton, Astronomic timescale for the Pliocene Atlantic $d^{18}O$ and dust flux records of Ocean Drilling Program Site 659, Paleoceanography 9 (1994) 619–638.

[82] J.B. Moody, L.R. Chaboudy, T.R. Worsley, Pacific pelagic phosphorus accumulation during the last 10 M.y., Paleoceanography 3 (1988) 113–136.

[83] G. Bohrmann, Zur Sedimentationsgeschichte von biogenem Opal im noerdlichen Nordatlantik und dem Europaeischen Nordmeer, Berichte aus dem Sonderforschungsbereich 313, Christian Albrechts Univ., Kiel, 9, 1988, 221 pp.

[84] T.R. Janecek, Data report: Late Neogene biogenic opal data for Leg 167 sites on the California margin, in: M. Lyle, I. Koizumi, C. Richter, T.C. Moore Jr. (Eds.), Proc. ODP, Sci. Results 167, Ocean Drilling Program, College Station, TX, 2000, pp. 213–214.

[85] R. Tiedemann, Acht Millionen Jahre Klimageschichte von Nordwest Afrika und Paläo-Ozeanographie des angrenzenden Atlanktis: hochauflösende Zeitreihen von ODP-Sites 658–661, Berichte-Reports, Geol.-Paläontologisches Institut, Univ. Kiel, 46, 1991, 190 pp.

[86] M.E. Pérez, H.-L. Lin, C.B. Lange, R. Schneider, Pliocene–Pleistocene opal records off southwest Africa, sites 1082 and 1084: a comparison of analytical techniques, in: G. Wefer, W.H. Berger, C. Richter (Eds.), Proc. ODP, Sci. Results, Ocean Drilling Program, College Station, TX, 2001, pp. 1–16, [Online]. Available from World Wide Web: http://www-odp.tamu.edu/publications.

[87] D. Eisma, S.J. van der Goast, Determination of opal in marine sediments by x-ray diffraction. Neth. J. Sea Res. 5 (1971) 382–389.

[88] G. Kuhn, B. Diekmann, Late Quaternary variability of ocean circulation in the southeastern South Atlantic inferred from the terrigenous sediment record of a drift deposit in the southern Cape Basin (ODP Site 1089), Palaeogeogr. Palaeoclimatol, Paleoecol. 182 (2002) 287–303.